

LYMPHOID NEOPLASIA

High frequency of inactivating tetraspanin *CD37* mutations in diffuse large B-cell lymphoma at immune-privileged sites

Suraya Elfrink,^{1,*} Charlotte M. de Winde,^{1,*} Michiel van den Brand,^{2,*} Madeleine Berendsen,² Margaretha G. M. Roemer,³ Frank Arnold,¹ Luuk Janssen,¹ Alie van der Schaaf,¹ Erik Jansen,¹ Patricia J. T. A. Groenen,² Astrid Eijkelenboom,² Wendy Stevens,⁴ Corine J. Hess,⁴ J. Han van Krieken,² Joost S. P. Vermaat,⁵ Arjen H. G. Cleven,⁶ Ruben A. L. de Groen,^{5,6} Viviana Neviani,⁷ Daphne de Jong,³ Sjoerd van Deventer,^{1,†} Blanca Scheijen,^{2,†} and Annemiek B. van Spriel¹

¹Department of Tumor Immunology and ²Department of Pathology, Radboud Institute for Molecular Life Sciences, Radboud University Medical Center, Nijmegen, The Netherlands; ³Amsterdam UMC-Vrije Universiteit Amsterdam, Department of Pathology and Cancer Center Amsterdam, Amsterdam, The Netherlands; ⁴Department of Hematology, Radboud University Medical Center, Nijmegen, The Netherlands; ⁵Department of Hematology and ⁶Department of Pathology, Leiden University Medical Center, Leiden, The Netherlands; and ⁷Crystal and Structural Chemistry, Department of Chemistry, Bijvoet Center for Biomolecular Research, Utrecht University, Utrecht, The Netherlands

KEY POINTS

- Loss-of-function mutations in *CD37* occur predominantly in diffuse large B-cell lymphoma at immune-privileged sites.
- *CD37*-mutated lymphoma B cells show impaired *CD37* cell-surface localization, which may have implications for anti-*CD37* therapies.

Tetraspanin *CD37* is predominantly expressed on the cell surface of mature B lymphocytes and is currently being studied as novel therapeutic target for B-cell lymphoma. Recently, we demonstrated that loss of *CD37* induces spontaneous B-cell lymphoma in *Cd37*-knockout mice and correlates with inferior survival in patients with diffuse large B-cell lymphoma (DLBCL). Here, *CD37* mutation analysis was performed in a cohort of 137 primary DLBCL samples, including 44 primary immune-privileged site-associated DLBCL (IP-DLBCL) samples originating in the testis or central nervous system. *CD37* mutations were exclusively identified in IP-DLBCL cases (10/44, 23%) but absent in non-IP-DLBCL cases. The aberrations included 10 missense mutations, 1 deletion, and 3 splice-site *CD37* mutations. Modeling and functional analysis of *CD37* missense mutations revealed loss of function by impaired *CD37* protein expression at the plasma membrane of human lymphoma B cells. This study provides novel insight into the molecular pathogenesis of IP-DLBCL and indicates that anti-*CD37* therapies will be more beneficial for DLBCL patients without *CD37* mutations. (*Blood*. 2019;134(12):946-950)

Introduction

Diffuse large B-cell lymphoma (DLBCL) is the most common type of B-cell non-Hodgkin lymphoma. Several genetic aberrations are known to underlie DLBCL development and progression. Recently, we identified that *Cd37*-knockout mice spontaneously develop B-cell lymphoma.¹ Moreover, *CD37* protein expression has been reported to be an independent prognostic factor for patient outcome in R-CHOP (rituximab, cyclophosphamide, doxorubicin, vincristine, prednisone)-treated DLBCL patients.²

CD37 (Tspan-26), a member of the tetraspanin superfamily, is highly expressed on mature B lymphocytes³ and is currently studied as novel target for chimeric antigen receptor (CAR)-T cell therapy⁴ and antibody-based therapies for patients with relapsed/refractory non-Hodgkin lymphoma.^{5,6} Tetraspanins control the spatial distribution of membrane proteins through specific interactions with (immune-)receptors and signaling molecules, thereby facilitating intracellular signaling pathways.^{7,8} Tetraspanins are

associated with different malignancies,⁹ but the role of altered tetraspanin function in DLBCL pathogenesis is unclear.

This study evaluated the mutational status of the human *CD37* gene in DLBCL patients, particularly in DLBCL at immune-privileged sites (IP-DLBCL), including primary testis lymphoma (PTL) and primary central nervous system lymphoma (PCNSL). With functional analysis, the effect of identified *CD37* mutations on *CD37* protein expression at the cell membrane was studied.

Study design

Cases

The study was conducted with 137 archived primary DLBCL samples, including 44 IP-DLBCL. The discovery cohort included 31 DLBCL samples and 106 DLBCL samples were analyzed in the validation cohort. Samples were collected from multiple Dutch university hospitals (supplemental Table 1, available on the *Blood* Web site).

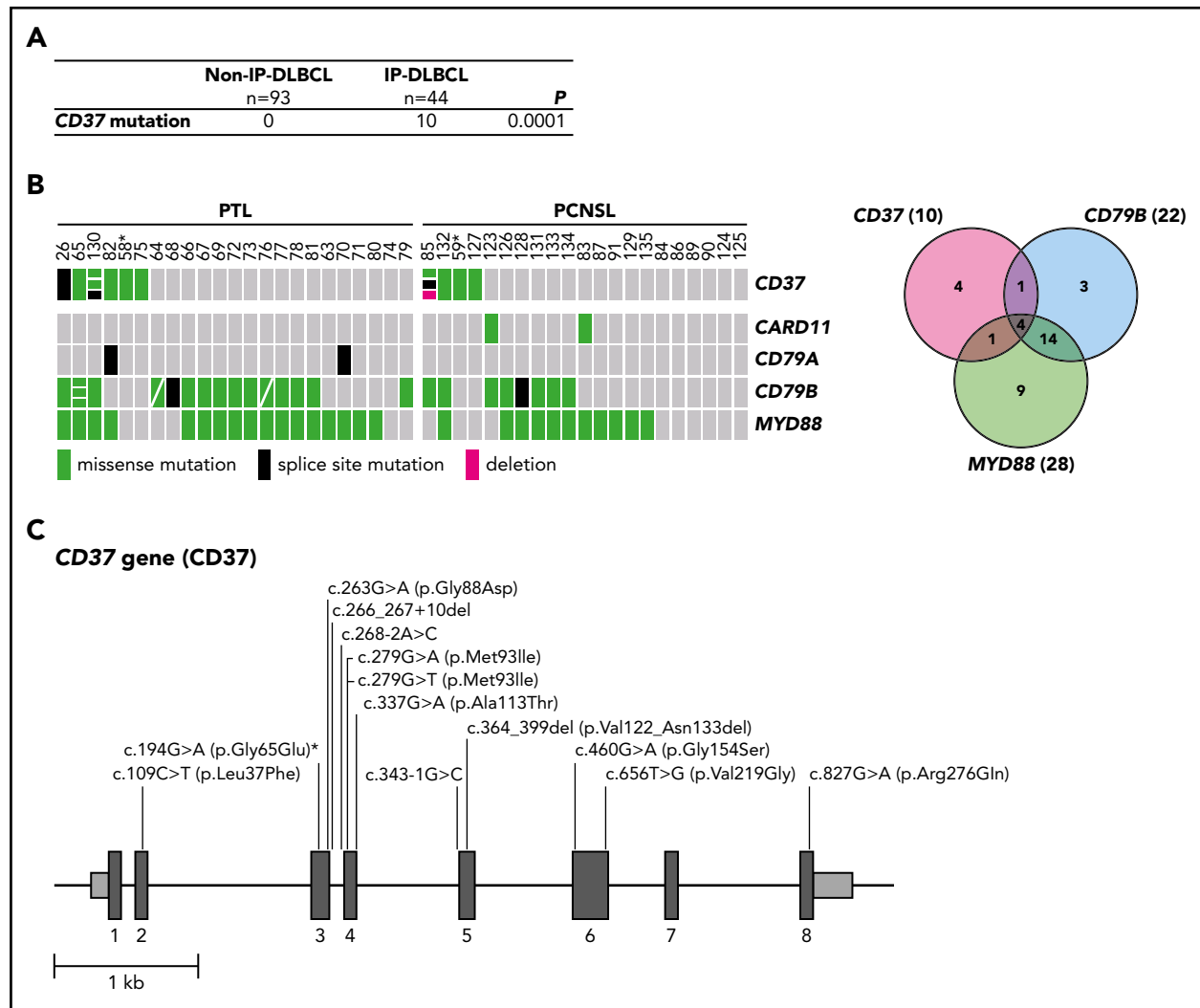


Figure 1. High frequency of mutated CD37 in IP-DLBCL. (A) Frequency of CD37 mutations in non-IP-DLBCL vs IP-DLBCL. The total number of lymphoma cases for each group is indicated. Numbers in the CD37 mutation row indicate the number of lymphoma cases carrying ≥ 1 CD37 mutation. P values were obtained using the Fisher's exact test. (B) OncoPrint (left) and Venn diagram (right) show the frequencies of CD37, CARD11, CD79A, CD79B, and MYD88 mutations in all IP-DLBCL cases studied (23 PTL and 21 PCNSL). Columns show individual tumors. Asterisk indicates samples from the same patient containing the CD37 germline mutation. Genetic details per mutation can be found in supplemental Table 2. Green, missense mutation; black, splice-site mutation; magenta, deletion; gray, no mutation. (C) Schematic representation of mutations detected in the CD37 gene. Dark gray boxes represent the coding sequence of CD37, light gray boxes are the noncoding sequence before exon 1 (begin) and after exon 8 (end), and black lines represent introns. Asterisk indicates the CD37 germline mutation.

Mutation analysis

CD37 mutation analysis of the discovery cohort was performed by amplicon-based sequencing with Ion Torrent and Sanger sequencing. For the validation cohort, single-molecule molecular inversion probe mutation analysis and sequencing with Ion Torrent included the CD37 gene and hotspot loci of CARD11, CD79A, CD79B, and MYD88.

Functional analysis of mutant CD37

The CD37-Gly88Asp-green fluorescent protein (GFP) and CD37-Gly65Glu-GFP mutant constructs were generated by introducing point mutations c.263G>A or c.194G>A in hCD37-wild-type (WT)-GFP¹ using site-directed mutagenesis. Human BJAB and OCI-Ly8 lymphoma B cells were transfected with the AMAXA Nucleofactor or the Neon transfection system and analyzed for CD37 protein expression and subcellular localization using western blot and confocal fluorescence microscopy.

Additional experimental details are provided in supplemental Materials and methods.

Results and discussion

In a discovery cohort of 31 DLBCL cases, including 5 PTL cases, CD37 mutations were analyzed. CD37 mutations were identified in 2 PTL cases, 1 harboring a missense mutation (c.263G>A (p.Gly88Asp)) and the other a splice-site mutation (c.343-1G>C), but none were identified in the non-IP-DLBCL samples (n = 26). To confirm this finding, a validation cohort consisting of 39 IP-DLBCL cases (18 PTL and 21 PCNSL) and 67 non-IP-DLBCL cases was analyzed for CD37 mutations along with CARD11, CD79A, CD79B, and MYD88 hotspot mutations (Figure 1; supplemental Table 2). In this analysis, we also included the 5 PTL cases from the discovery cohort. Besides confirmation of the 2 initially identified CD37 mutations, we uncovered 12 additional mutations (variant allele frequency 5.7% to 49%; Figure 1B-C).

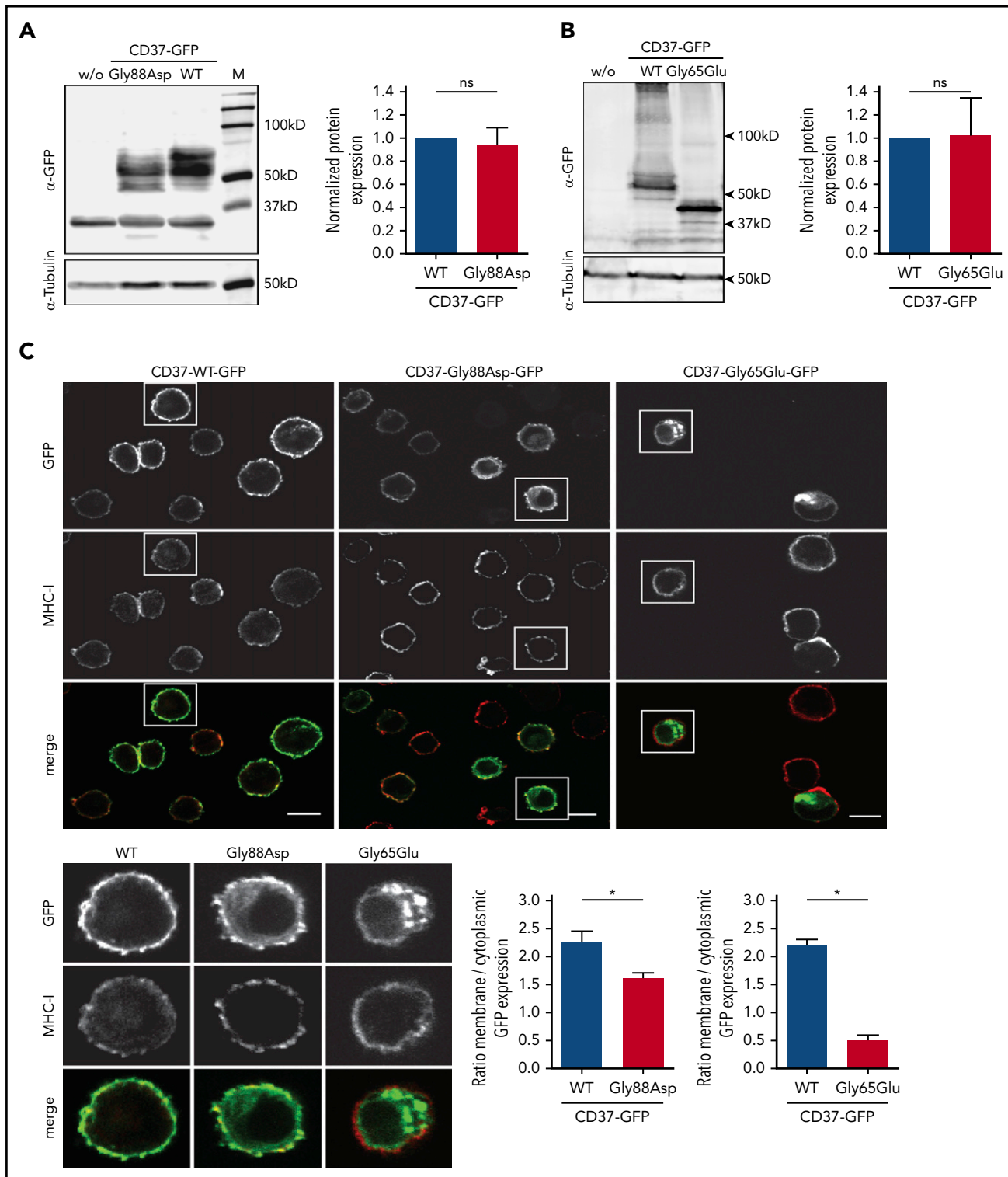


Figure 2. Mutations in CD37 cause aberrant CD37 glycosylation and localization. Western blot analysis of CD37 protein expression in BJAB lymphoma B cells transfected with CD37-WT-GFP, CD37-Gly88Asp-GFP (A), or CD37-Gly65Glu-GFP (B). Blots were probed with α -GFP to detect CD37-GFP expression (50-75 kDa; upper blot). α -Tubulin was used as a loading control (lower blot). Protein expression level of CD37-mutant-GFP was normalized to CD37-WT-GFP for each experiment ($n = 3$). ns, not significant ($P = .73$ [left], $P = .96$ [right]), paired t test. (C) Confocal microscopy images of BJAB cells expressing CD37-WT-GFP and CD37-Gly88Asp-GFP or CD37-Gly65Glu-GFP (green) costained for MHC-I (red) to identify the plasma membrane. Overview images (top) and single-cell images (bottom left) show representative cells of 3 independent experiments for both CD37-WT-GFP and CD37-mutant-GFP. Scale bar, 10 μ m. Ratio between membrane and cytoplasmic GFP expression was quantified from 10 representative cells of 3 independent experiments. * $P = .023$ (left), $P = .011$ (right), paired t test. All data represent mean \pm standard error of the mean.

Intriguingly, all *CD37* mutations were exclusively present in IP-DLBCL cases ($n = 10/44$, 23%); and none were present in the non-IP-DLBCL cases ($n = 0/93$; Fisher's exact test, $P = .0001$; Figure 1A). Mutation rates of frequently affected genes *CARD11* (5%), *CD79A* (5%), *CD79B* (50%), and *MYD88* (64%) in our cohort (Figure 1B; supplemental Table 2) were in line with other DLBCL studies.¹⁰⁻¹³ Whole-genome and exome sequencing studies of DLBCL report low mutation frequencies of *CD37*, ranging from no mutations to 8%.^{11,14-17}

The *CD37* mutations identified in the validation cohort were detected in 8 IP-DLBCL cases and included 9 missense mutations (c.109C>T (p.Leu37Phe), c.194G>A (p.Gly65Glu) [twice], c.279G>A (p.Met93Ile), c.279G>T (p.Met93Ile), c.460G>A, (p.Gly154Ser), c.656T>G (p.Val219Gly), c.337G>A (p.Ala113Thr), and c.827G>A (p.Arg276Gln)), 1 in-frame deletion (c.364_399del (p.Val122_Asn133del)), and 2 splice-site mutations (c.266_267+10del, c.268-2A>C) (Figure 1C; pathogenicity scores are listed in supplemental Table 2). Within 1 patient, missense mutation c.194G>A (p.Gly65Glu) was detected in 2 primary lymphoma specimens as well as healthy control tissue, but not described as a single-nucleotide polymorphism, indicating the presence of a *CD37* germline mutation. To the best of our knowledge, this is the first reported *CD37* germline mutation in humans.

To determine the effect of splice-site mutation c.343-1G>C, complementary DNA of this DLBCL sample was sequenced, which revealed an 11-bp deletion (supplemental Figure 1). This resulted in a frameshift in the *CD37* mRNA sequence, leading to a completely altered protein after transmembrane domain 3. Based on previous studies on tetraspanin *CD81* in B cells,¹⁸ this mutation is predicted to result in a nonfunctional *CD37* protein, since the essential extracellular domain 2 is truncated.¹⁹ Next, the *CD37* missense mutations and in-frame deletion were mapped onto the reported crystal structure of tetraspanin *CD81*²⁰ (supplemental Figure 2). Deletion c.364_399del (p.Val122_Asn133del) disrupts an important structural element of extracellular domain 2, namely the A helix, and is therefore also predicted to result in a nonfunctional *CD37* protein.¹⁹

To further assess whether the observed missense mutations resulted in *CD37* loss of function, we introduced 2 of the identified *CD37* mutations, c.263G>A (p.Gly88Asp) and c.194G>A (p.Gly65Glu), in human lymphoma B cells using a GFP expression vector. WT *CD37* protein appeared as 50- to 75-kDa bands on western blot (Figure 2A-B; supplemental Figure 3A) due to heavy glycosylation. Protein isoforms with the highest glycosylation state (± 70 kDa) were less pronounced in lymphoma B cells expressing mutant *CD37*-Gly88Asp-GFP (Figure 2A), and *CD37*-Gly65Glu-GFP showed a lower-molecular-weight band on western blot indicating a glycosylation defect (Figure 2B). Total *CD37*-GFP protein levels of both mutants were similar to *CD37*-WT-GFP (Figure 2A-B).

Next, the subcellular localization of the *CD37* mutants was determined using confocal microscopy. Lymphoma B cells expressing the *CD37*-GFP mutants had significantly lower cell membrane expression and more retention of intracellular *CD37* protein than cells expressing *CD37*-WT-GFP (Figure 2C; supplemental Figure 3B). Moreover, *CD37*-Gly88Asp had a dominant-negative effect on the membrane expression of *CD37*-WT protein (supplemental Figure 4). These data indicate that these missense mutations

result in defective glycosylation and trafficking of *CD37* in human lymphoma B cells, which corresponds to the reported role of glycosylation as a sorting signal for protein transport to the plasma membrane.²¹ Moreover, modification of cell-surface proteins by defective glycosylation frequently contributes to cancer development by enhancing invasive growth and tumor cell migration.²²

We previously showed that loss of *CD37* results in increased interleukin-6 signaling and STAT3 activation,¹ which are both known to be involved in the pathogenesis of hematological malignancies.²³ *MYD88* mutations also stimulate cell survival by promoting JAK/STAT3 signaling and interleukin-6 secretion, suggesting a similar phenotype.²⁴ As proposed for *MYD88* and *CD79B* mutations in IP-DLBCL,¹² mutations in *CD37* could therefore provide a survival advantage in the otherwise stimulus-poor environment of immune-privileged sites.

Seven out of 9 evaluable cases with a *CD37* mutation did not express *CD37* protein (supplemental Figure 5 and supplemental Table 1). Since immunohistochemistry does not distinguish between cell-surface and cytosolic expression, the importance of *CD37* in DLBCL biology^{1,2} is likely underestimated. Moreover, the recent identification of loss of *CD19* expression as a mechanism underlying disease relapse upon *CD19* CAR-T cell therapy²⁵ emphasizes the need to investigate *CD37* surface expression in hematologic malignancies prior to the use of novel *CD37* CAR-T cell therapies.

In conclusion, inactivating *CD37* mutations occur predominantly in IP-DLBCL and lead to aberrant *CD37* cell-surface expression. This study provides novel molecular insight into DLBCL at immune-privileged sites and indicates that *CD37*-based therapies are more likely to be beneficial for DLBCL patients that harbor no *CD37* mutations.

Acknowledgments

The authors thank Piet Gros (Department of Chemistry, Utrecht University) for his valuable help with the modeling studies and Shannon van Lent-van Vliet and Sanne Sweegers (Department of Pathology, Radboudumc) for their valuable help with the single-molecule molecular inversion probe analysis. The authors apologize to all authors whose work could not be cited due to space limitations.

S.E. is supported by a Radboudumc grant. C.M.d.W. is supported by a Rubicon Fellowship from The Netherlands Organization for Scientific Research (019.162LW.004). J.V., A.C., and R.G. are supported by research funding from Stichting Fonds Oncologie Holland. A.B.v.S. is recipient of a Netherlands Organization for Scientific Research grant (NWO-ALW VIDI grant 864.11.006), a Netherlands Organization for Scientific Research Gravitation Programme 2013 grant (ICI-024.002.009), and a Dutch Cancer Society grant (KUN2014-6845) and was awarded an European Research Council Consolidator grant (Secret Surface, 724281).

Authorship

Contribution: S.E., C.M.d.W., M.v.d.B., S.v.D., B.S., and A.B.v.S. designed the study; S.E., C.M.d.W., M.v.d.B., S.v.D., and A.B.v.S. wrote the manuscript; M.v.d.B., C.J.H., W.S., M.G.M.R., D.d.J., J.S.P.V., A.H.G.C., and B.S. collected DLBCL tissue and corresponding pathological information; S.E., C.M.d.W., M.v.d.B., E.J., A.v.d.S., S.v.D., P.J.T.A.G., A.E., R.A.L.d.G., and M.B. performed mutation analysis; S.E., F.A., L.J., and S.v.D. performed functional in vitro experiments; V.N.

performed CD37 modeling studies; and J.H.v.K., S.v.D., B.S., and A.B.v.S. supervised the work.

Conflict-of-interest disclosure: The authors declare no competing financial interests.

ORCID profiles: C.M.d.W., 0000-0002-8318-4612; M.v.d.B., 0000-0001-8871-6254; P.J.T.A.G., 0000-0003-4314-228X; A.E., 0000-0001-8264-8131; J.H.v.K., 0000-0002-8105-0450; V.N., 0000-0002-5729-3639; D.d.J., 0000-0002-9725-4060; A.B.v.S., 0000-0002-3590-2368.

Correspondence: Annemiek B. van Spriël, Department of Tumor Immunology, Radboud Institute for Molecular Life Sciences, Radboud University Medical Center, Geert Grooteplein-Zuid 26-28, 6525 GA Nijmegen, The Netherlands; e-mail: annemiek.vanspriel@radboudumc.nl.

Footnotes

Submitted 18 April 2019; accepted 20 July 2019. Prepublished online as *Blood* First Edition paper, 31 July 2019; DOI 10.1182/blood.2019001185.

*S.E., C.M.d.W., and M.v.d.B. contributed equally to this study.

†S.v.D. and B.S. contributed equally to this study.

The online version of this article contains a data supplement.

The publication costs of this article were defrayed in part by page charge payment. Therefore, and solely to indicate this fact, this article is hereby marked "advertisement" in accordance with 18 USC section 1734.

REFERENCES

- de Winde CM, Veenbergen S, Young KH, et al. Tetraspanin CD37 protects against the development of B cell lymphoma. *J Clin Invest*. 2016;126(2):653-666.
- Xu-Monette ZY, Li L, Byrd JC, et al. Assessment of CD37 B-cell antigen and cell of origin significantly improves risk prediction in diffuse large B-cell lymphoma. *Blood*. 2016;128(26):3083-3100.
- Barrena S, Almeida J, Yunta M, et al. Aberrant expression of tetraspanin molecules in B-cell chronic lymphoproliferative disorders and its correlation with normal B-cell maturation. *Leukemia*. 2005;19(8):1376-1383.
- Scarfò I, Ormhøj M, Frigault MJ, et al. Anti-CD37 chimeric antigen receptor T cells are active against B- and T-cell lymphomas. *Blood*. 2018;132(14):1495-1506.
- Robak T, Hellmann A, Kloczko J, et al. Randomized phase 2 study of otlertuzumab and bendamustine versus bendamustine in patients with relapsed chronic lymphocytic leukaemia. *Br J Haematol*. 2017;176(4):618-628.
- Stathis A, Flinn IW, Madan S, et al. Safety, tolerability, and preliminary activity of IMG529, a CD37-targeted antibody-drug conjugate, in patients with relapsed or refractory B-cell non-Hodgkin lymphoma: a dose-escalation, phase I study. *Invest New Drugs*. 2018;36(5):869-876.
- Rubinstein E, Le Naour F, Lagaudrière-Gesbert C, Billard M, Conjeaud H, Boucheix C. CD9, CD63, CD81, and CD82 are components of a surface tetraspan network connected to HLA-DR and VLA integrins. *Eur J Immunol*. 1996;26(11):2657-2665.
- Zuidscherwoude M, Göttfert F, Dunlock VME, Figdor CG, van den Bogaart G, van Spriël AB. The tetraspanin web revisited by super-resolution microscopy. *Sci Rep*. 2015;5(1):12201.
- Hemler ME. Tetraspanin proteins promote multiple cancer stages. *Nat Rev Cancer*. 2014;14(1):49-60.
- Reddy A, Zhang J, Davis NS, et al. Genetic and functional drivers of diffuse large B cell lymphoma. *Cell*. 2017;171(2):481-494.e15.
- Chapuy B, Stewart C, Dunford AJ, et al. Molecular subtypes of diffuse large B cell lymphoma are associated with distinct pathogenic mechanisms and outcomes. *Nat Med*. 2018;24(5):679-690.
- Kraan W, Horlings HM, van Keimpema M, et al. High prevalence of oncogenic MYD88 and CD79B mutations in diffuse large B-cell lymphomas presenting at immune-privileged sites. *Blood Cancer J*. 2013;3(9):e139.
- Bruno A, Boisselier B, Labreche K, et al. Mutational analysis of primary central nervous system lymphoma. *Oncotarget*. 2014;5(13):5065-5075.
- Zhang J, Grubor V, Love CL, et al. Genetic heterogeneity of diffuse large B-cell lymphoma. *Proc Natl Acad Sci USA*. 2013;110(4):1398-1403.
- Morin RD, Mungall K, Pleasance E, et al. Mutational and structural analysis of diffuse large B-cell lymphoma using whole-genome sequencing. *Blood*. 2013;122(7):1256-1265.
- Park HY, Lee S-B, Yoo H-Y, et al. Whole-exome and transcriptome sequencing of refractory diffuse large B-cell lymphoma. *Oncotarget*. 2016;7(52):86433-86445.
- Schmitz R, Wright GW, Huang DW, et al. Genetics and pathogenesis of diffuse large B-cell lymphoma. *N Engl J Med*. 2018;378(15):1396-1407.
- Vences-Catalán F, Kuo C-C, Sagi Y, et al. A mutation in the human tetraspanin CD81 gene is expressed as a truncated protein but does not enable CD19 maturation and cell surface expression. *J Clin Immunol*. 2015;35(3):254-263.
- Stipp CS, Kolesnikova TV, Hemler ME. Functional domains in tetraspanin proteins. *Trends Biochem Sci*. 2003;28(2):106-112.
- Zimmerman B, Kelly B, McMillan BJ, et al. Crystal structure of a full-length human tetraspanin reveals a cholesterol-binding pocket. *Cell*. 2016;167(4):1041-1051.e11.
- Lodish H, Berk A, Kaiser CA, et al. Moving proteins into membranes and organelles. *Molecular Cell Biology*. 8th ed. New York: W.H. Freeman; 2016.583-630.
- Gill DJ, Tham KM, Chia J, et al. Initiation of GalNAc-type O-glycosylation in the endoplasmic reticulum promotes cancer cell invasiveness. *Proc Natl Acad Sci USA*. 2013;110(34):E3152-E3161.
- Burger R. Impact of interleukin-6 in hematological malignancies. *Transfus Med Hemother*. 2013;40(5):336-343.
- Ngo VN, Young RM, Schmitz R, et al. Oncogenically active MYD88 mutations in human lymphoma. *Nature*. 2011;470(7332):115-119.
- Orlando EJ, Han X, Tribouley C, et al. Genetic mechanisms of target antigen loss in CAR19 therapy of acute lymphoblastic leukemia. *Nat Med*. 2018;24(10):1504-1506.